



Peroxide degradation of azo dye using hydrothermally synthesized Cu-L zeolite as high performance catalyst

Jiajia Dong, Hexin Dong, Li Han, Bei Fu, Yiliang Chen, Yuzhong Zhan*

School of Chemical and Energy Engineering, Zhengzhou University, Kexue Road, Zhengzhou 450001, P.R. China, Tel./Fax: +86 0371 67781025; emails: jiajiaxiangfeng@163.com (J. Dong), dhx719@zzu.edu.cn (H. Dong), lihan@zzu.edu.cn (L. Han), twinsfubei@126.com (B. Fu), liangchen@zzu.edu.cn (Y. Chen), zhanyz@zzu.edu.cn (Y. Zhan)

Received 6 December 2013; Accepted 27 June 2014

ABSTRACT

Cu-L zeolites synthesized hydrothermally with various Cu contents were characterized by X-ray diffractometer, SEM, and Fourier transform infrared, and their catalytic performance was evaluated using Acid Scarlet as a model compound. The effects of various parameters such as Cu content, temperature, initial pH, catalyst, and H₂O₂ dosage, initial dye concentration, and inorganic salts on the degradation of dye were studied. The results showed that adjusting Cu content could result in high catalytic activity, and Cu species highly dispersed in the channels of zeolite L played a crucial role in the catalytic activity. The diffusion limitation and adsorption of larger Acid Scarlet molecule did not influence the degradation. For the best catalyst, Acid Scarlet of 400 mg/L could be degraded effectively in 120 min at 50°C under low catalyst and low H₂O₂ dosage. The degradation could be carried out in a wide pH range. Under near-neutral conditions the catalyst showed the highest catalytic activity. The existence of NaCl or Na₂SO₄ obviously decreased the initial rate of Acid Scarlet degradation, but did not influence the eventual decolorization efficiencies significantly. The catalyst appeared to have good stability and less Cu was leached out during the dye degradation.

Keywords: Hydrothermal synthesis; Cu-L zeolite; Advanced oxidation process; Azo dye; Peroxide degradation; Diffusion limitation

1. Introduction

Generally, conventional biological processes cannot treat wastewater containing biorefractory or toxic chemicals such as dyes, phenol and its derivatives, pharmaceuticals and intermediates, and pesticides. Although some physicochemical technologies such as adsorption, coagulation, and membrane separation have been demonstrated as effective, these methods merely transfer pollutants from one medium to

another requiring further treatment [1–3]. So-called advanced oxidation processes (AOPs), which are based upon the generation of hydroxyl radicals, offer potentials of destructing organic pollutants ultimately to water, carbon dioxide, and other harmless small molecules without secondary pollution [4,5]. These environmentally friendly methods are especially suitable for removing toxic organic chemicals. Among the various AOPs, the classical Fenton's reagent consisting of a homogeneous solution of Fe²⁺/H₂O₂ may be the most extensively studied system [6–9]. However, two

*Corresponding author.

major drawbacks limit its applications: the pH of operation should be strictly controlled around pH 3; and large amounts of sludge require further treatment [10,11]. To overcome these disadvantages, considerable attentions have been turned to heterogeneous Fe-containing catalysts [11,12]. However, Cu-containing heterogeneous catalysts have attracted increasing attention in recent years because Cu species can also undergo Fenton-like reaction and the reaction can usually be operated under a wider pH range [13–22].

The major way to prepare heterogeneous catalysts is to disperse active species on porous supports with huge specific surface areas. This strategy may result in more active sites, and high catalytic activity is therefore expected. The same method was also applied in the preparation of heterogeneous Fenton's catalysts. Apparently, support materials can significantly influence the catalytic performance [23]. Up to now, many supports have been investigated, but the researches mainly focus on carbon materials [13,24], clays [25–28], and zeolites [25,27]. Zeolites are crystalline aluminosilicates with uniform pore of molecular dimensions and are widely used as catalysts and supports. The characters of zeolites, such as framework type, channel structure, opening diameter, Si/Al ratio, cation, and doping elements, determine their catalytic performance. Although over the past decades hundreds of zeolites were synthesized, only several such as zsm-5 [29], Y [30], 13X [15], beta [31], and SAB-15 mesoporous zeolite [21] have been investigated in Fenton's processes. Natural zeolites have also been used as supports in heterogeneous Fenton processes. Recently, an iron-loaded natural zeolite was being found to be effective to degradation and debromination of 2,4,6-tribromophenol via a Fenton-like process in the presence of reducing agents such as ascorbic acid or hydroxylamine [32]. Zero-valent iron loaded on a natural zeolite (clinoptilolite) was demonstrated as a potent low leaching Fenton catalyst for the degradation of benzene [33]. In addition, zeolites are microporous materials with the opening diameter generally less than 1 nm, hence smaller molecules can diffuse into zeolite channels, but larger molecules like many azo dyes cannot. Hence, an important question arises whether the diffusion and the further adsorption of pollutants influence their degradation. Unfortunately, this question has received little attention.

Zeolite L is a middle-silica zeolite with one-dimension channel of 0.71 nm [34]. In this study, we hydrothermally synthesized a series of Cu-L zeolites with various Cu contents and evaluated their catalytic performance using an azo dye Acid Scarlet as a model compound. The catalysts synthesized were also characterized by X-ray diffractometer (XRD), SEM, and

Fourier transform infrared (FTIR). The results showed that adjusting Cu content could prepare Cu-L zeolites not only with high activity but also with an effective use of H_2O_2 .

2. Materials and methods

2.1. Materials

Acid Scarlet (C.I. 16,150, commercial grade) was purchased from Shanghai Huyu Biological Technology Co. Ltd, China. The molecular structure is shown in Fig. 1. Fumed silica (commercial grade) was purchased from Suzhou Donghua Fangui Co. Ltd, China. Other chemical reagents used were of analytical grade.

2.2. Synthesis and characterization of Cu-L zeolites

Cu-L zeolites were synthesized hydrothermally in 100 mL Teflon-lined stainless steel autoclaves. The initial gel compositions (mole ratio) were $4.2K_2O:Al_2O_3:14SiO_2:189H_2O:nCu$, where n was 0, 0.005, 0.02, 0.1, 0.2, 0.5, and 1.0, and the corresponding products synthesized were named as S0, S1, S2, S3, S4, S5, and S6, respectively. The initial gel was obtained by mixing and stirring for 30 min the fumed silica with potassium aluminate solution prepared by dissolving $Al(OH)_3$ in KOH solution. Then $Cu(NO_3)_2$ solution was added and the gel was continuously stirred for another 30 min. The crystallization was carried out in static condition at $150^\circ C$ for 24 h. The solid product was filtered, washed with deionized water to about pH 8, and dried at $110^\circ C$ for 4 h.

XRD data were collected on a Y-2000 automated XRD system (Dandong Aolong Radiative Instrument Co. Ltd, China) with Cu $K\alpha$ radiation. FTIR spectra were obtained on a WQF-510 FTIR spectrometer

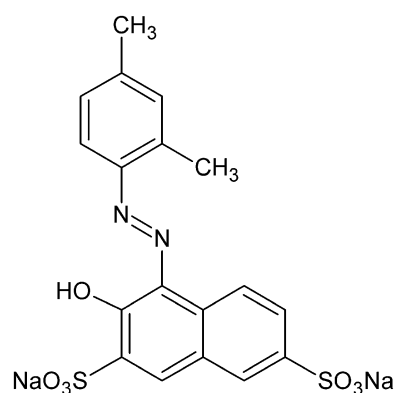


Fig. 1. Molecular structure of Acid Scarlet.

(Beijing Rayleigh Analytical Instrument Corp., China) using the KBr disc method. SEM images were recorded on a JSM-7500F (Jeol, Japan). The Cu content of the samples and the leaching Cu concentration were measured by a TAS-986 atomic absorption spectrometer (Beijing Purkinje General Instrument Co. Ltd, China).

2.3. Experiments of dye degradation

The catalytic degradation of dye solution was carried out in a 250 mL conical flask fixed in a constant temperature water bath shaker. In a typical run, 50 mg as-synthesized samples were added into a 50 mL solution of 200 mg/L Acid Scarlet. When the temperature was stable at 50°C, 1 mL 3% H₂O₂ (a 10-time diluted solution of 30% H₂O₂) was added and the degradation began. In this case, the dosage of catalyst was 1 g/L, and H₂O₂ was 17.6 mM/L. At the given time intervals, 4 mL solution was taken out and centrifuged to remove the residual catalyst. The concentration of dye was analyzed using an SP-756PC UV-vis spectrophotometer (Shanghai Spectrum Instrument Co. Ltd, China). The decolorization efficiency was calculated by the following equation:

$$\text{Decolorization efficiency} = [(A_0 - A_t)/A_0] \times 100\%$$

where A_0 is the initial absorbance, A_t is the absorbance at time t .

3. Results and discussion

3.1. Characterization of Cu-L zeolites

Basically, there are three ways to load metal species on zeolites: ion-exchange, precipitation, or direct hydrothermal synthesis. For direct synthesis, the addition of metal salts to synthesis system may interfere with the crystallization of desired zeolites. However, our results showed that adding an appropriate amount of Cu(NO₃)₂ to the synthesis gels did not influence the production of zeolite L, and the Cu-L zeolites with various Cu contents (S1–S5) were synthesized successfully. The XRD patterns closely agree with the literatures (Fig. 2) [35]. These Cu-L zeolites were of similar crystallinity to L zeolite (S0) synthesized without adding Cu(NO₃)₂, except one product (S3) containing a little impurity identified as hydrogen potassium silicate (PDF 43-0,29). The Cu contents of the Cu-L zeolites increased with the increase of Cu(NO₃)₂. But adding an excessive amount of Cu(NO₃)₂ to the synthesis gels obstructed the crystallization of

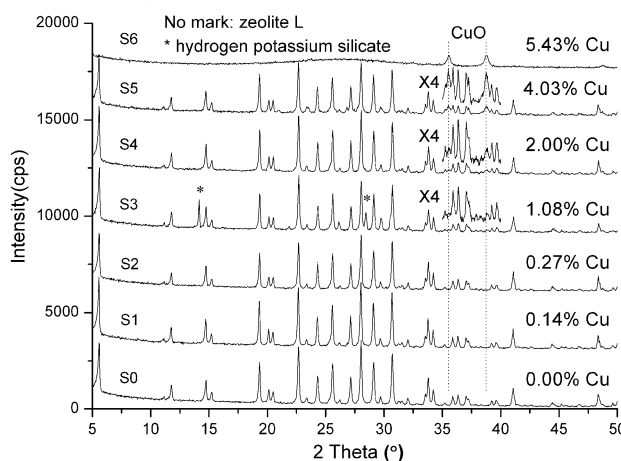


Fig. 2. XRD patterns of hydrothermally synthesized products.

zeolite L. In this case, the product was amorphous silica–alumina gel containing CuO nanoparticles because this sample (S6) only showed wide characteristic peaks of CuO (Fig. 2).

Copper species in Cu-L was responsible for the catalytic performance (see Section 3.2.1). In the as-synthesized Cu-L zeolites, copper species may exist in three types: Cu(II) partially replacing Al(III) into zeolite framework, Cu²⁺ partially exchanging K⁺, or loading in zeolite channels as CuO. Comparing the XRD patterns of zeolite Cu-L (samples S1–S5) and zeolite L (sample S0) showed no observable difference in the peak positions, implying Cu may mainly exist as CuO in the channels (Fig. 2). However, for the Cu-L samples with lower Cu content (S1 and S2) no CuO peaks existed in the XRD patterns, suggesting that CuO may disperse in the zeolite channels as the mono molecular layer. With the increase of Cu content (S3), slight CuO peaks appeared, indicating that the threshold value of mono molecular layer reached and CuO crystal began forming. Further increasing Cu content, weak but obvious peaks of CuO could be observed (Fig. 2).

FTIR spectra were also recorded for the structural characterization of the samples (Fig. 3). It is found that the FTIR spectrum of sample S0 matches very well with those of zeolite L reported in literatures. Characteristic peaks of zeolite L including T-O bending at 440 and 478/cm, D-6 ring at 609 and 580/cm, symmetric stretch at 727 and 779/cm, and asymmetric stretch at about 1,100/cm [36,37], approve the successful synthesis of zeolite L. Comparing the Cu-L samples (S1–S5) with the L sample (S0), neither new peaks nor peaks shifts were observed, indicating that Cu species did not influence the framework structure of

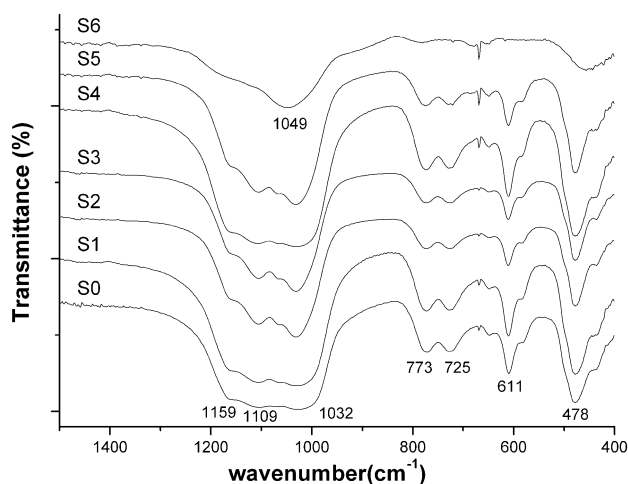


Fig. 3. FTIR spectra of hydrothermally synthesized products.

L zeolite. For sample S6, which was amorphous silica–alumina gel containing CuO nanoparticles, no zeolite peaks appeared, and the strong peak at about 1,050/cm and wide weak peak at 453/cm could attribute to the Si–O adsorption of silica-alumina gel and Cu–O adsorption of CuO, respectively [38].

Adding an appropriate amount of $\text{Cu}(\text{NO}_3)_2$ to the initial gels did not influence the crystal size and morphology of zeolite L significantly either. The products were still cylindrical like the typical zeolite L by conventional synthesis, seemingly with flatter end face (Fig. 4). No other particles were observed attaching on the Cu-L zeolite crystals. Sample S6, which appeared

as aggregates of small particles, was of the typical morphology of amorphous silica–alumina gel.

3.2. Effect of various parameters on the degradation of Acid Scarlet

3.2.1. Effect of Cu contents and temperature

The degradation of Acid Scarlet at 30°C showed that sample S3 exhibited much higher catalytic activity than the other samples and the decolorization efficiency at 120 min reached at 92% (Fig. 5(a)). As mentioned above, sample S3 may have a critical Cu content and the most catalytic sites. The samples (S1 and S2) with lower Cu contents exhibited lower activity for the smaller catalytic sites. Nevertheless, the samples (S4 and S5) with higher Cu contents also exhibited lower activity because the formation of CuO crystal may partly cover the catalytic sites or block the channels obstructing the contact of reactants with catalytic sites. For the zeolite L (S0) without Cu, the decolorization efficiency at 120 min was only 15%, clearly indicating that Cu acted as the catalytic active species in the peroxide degradation. On the other hand, L-zeolite structure may play an important role in the dye degradation, because the sample S6, which contained Cu but without L-zeolite structure, showed some degree activity but rather lower than that of the most Cu-L samples.

When raising the temperature to 50°C, the catalytic activity for all samples is enhanced (Fig. 5(b)). Sample S3 was still the most active catalyst and the decolorization efficiencies after only 15 min reached at 83%

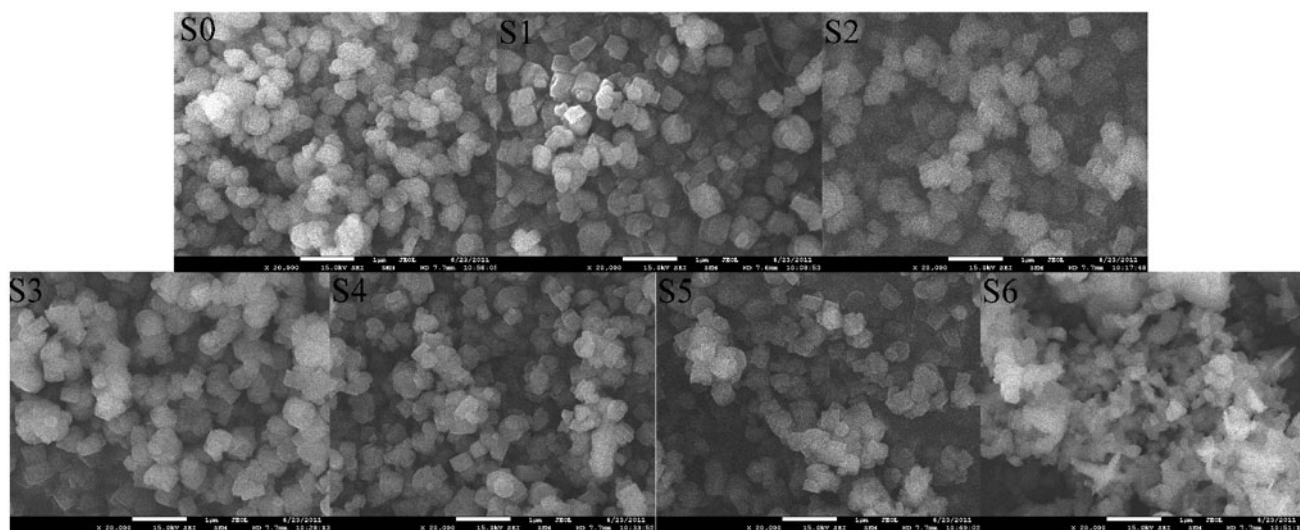


Fig. 4. SEM images of hydrothermally synthesized products.

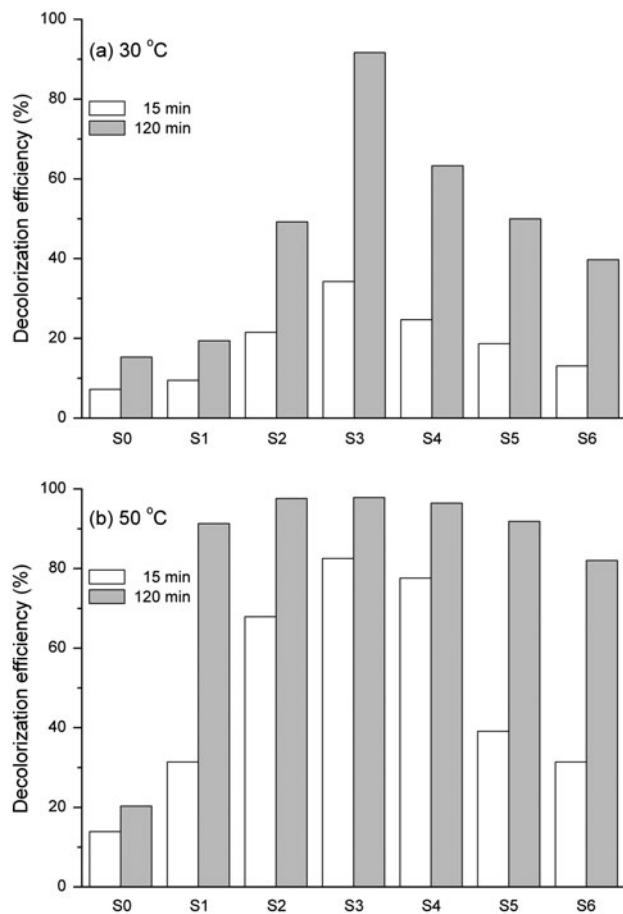


Fig. 5. Effect of Cu content and temperature on the degradation of Acid Scarlet (dye 200 mg/L, cat. 1 g/L, H_2O_2 17.6 mM, pH 6.5).

and after 120 min reached at 98%. This suggested that the Cu-L zeolite was of excellent catalytic performance, especially when considering the low dosage of catalyst and H_2O_2 and the relatively high concentration of dye. In the following sections we only show the results of sample S3, the best catalyst.

3.2.2. Effect of catalyst dosage

The effect of catalyst dosage on the degradation is shown in Fig. 6. The oxidizing ability of H_2O_2 alone was weak and the decolorization efficiency at 120 min was less than 10%. When adding 1 g/L Cu-L catalyst to the dye solution, the decolorization efficiency reached at 59% at 15 min and 98% at 120 min, indicating the catalyst was highly active and catalyzed H_2O_2 producing hydroxyl radicals, the extremely strong oxidizers. However, further increasing the catalyst to 2 and 4 g/L decreased the decolorization efficiencies

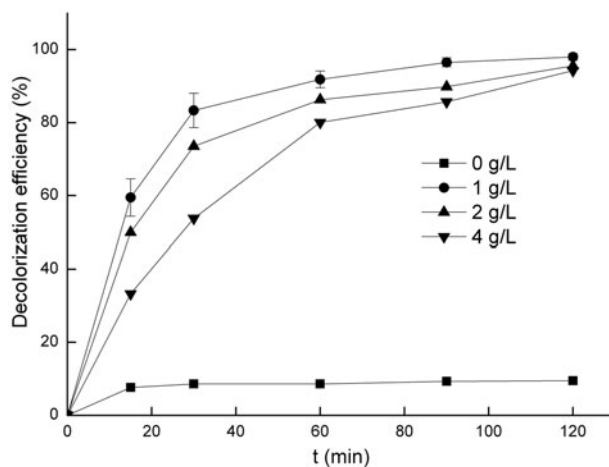


Fig. 6. Effect of catalyst dosage on the degradation of Acid Scarlet (temp. 50 °C, dye 400 mg/L, H_2O_2 17.6 mM, pH 6.5).

slightly. This phenomenon has been reported [39,40] and may be caused by several reasons. One possible reason is that the excessive catalyst may promote the decomposition of H_2O_2 due to the high catalytic activity, which results in ineffective use of H_2O_2 .

3.2.3. Effect of dye initial concentration

When the dye initial concentration increased from 200 to 600 mg/L, the decolorization efficiency decreased significantly from 83 to 33% at 15 min, but it decreased only from 98 to 95% at 120 min, indicating the catalyst could be used to treat dye wastewater with a high concentration (Fig. 7). However, the

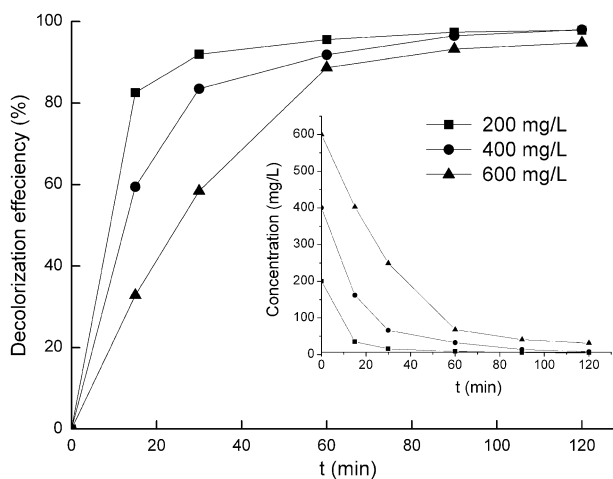


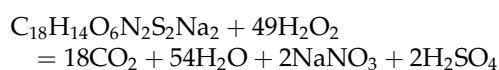
Fig. 7. Effect of dye initial concentration on the degradation of Acid Scarlet (temp. 50 °C, cat. 1 g/L, H_2O_2 17.6 mM, pH 6.5).

remaining dye after degradation was 4.3 mg/L for 200 mg/L initial concentration, and it reached at 7.9 mg/L for 400 and 31.3 mg/L for 600 mg/L. Hence, for higher dye concentrations, the degradation process may require more H_2O_2 dosage and longer reaction time.

3.2.4. Effect of H_2O_2 dosage

Without H_2O_2 the decolorization efficiency was only about 10% at 120 min, indicating that the adsorption amount of Acid Scarlet on the catalyst was insignificant. In the presence of 8.8 mM H_2O_2 , the decolorization efficiency increased drastically to 88% at only 15 min and about 98% at 120 min. Increasing H_2O_2 from 8.8 to 17.6 mM, 35.2, and 52.7 mM, although at 120 min all decolorization efficiencies were about 98%, at 15 min they decreased from 88 to 82%, 49, and 49%, respectively, indicating that the addition of excess H_2O_2 decreased the initial reaction rate of decolorization (Fig. 8). This phenomenon can be explained by the scavenging effect of H_2O_2 , which decreases the number of hydroxyl radicals in the solution [21,41].

The effective use of H_2O_2 is economically important because it is directly related to the running costs of wastewater treatment. However, H_2O_2 /pollutant molar ratios reported in literatures were usually much higher than the theoretical demand, meaning that a large amount of H_2O_2 was ineffectively used [42]. In this study, the overall stoichiometry of H_2O_2 completely degrading Acid Scarlet can be written as:



According to this equation, the degradation of 1 M Acid Scarlet needs 49 M H_2O_2 theoretically. Thus, the degradation of 50 mL solution of 200 mg/L Acid Scarlet needs 1.2 mL H_2O_2 of 3% (21.1 mM H_2O_2) used for this study. The addition of 8.8 and 17.6 mM to a reaction system was only about 42 and 83% of the theoretical value, respectively, and both decolorization efficiencies reached at about 98% at 120 min, indicating a very effective use of H_2O_2 when using the as-synthesized Cu-L as the catalyst.

The UV–visible absorption spectra were also recorded during the dye degradation (Fig. 9). Before degradation, the spectrum of Acid Scarlet consisted of two main characteristic absorption bands. One was in a visible region (488 nm), which was attributed to the chromophore-containing azo linkage of the Acid Scarlet molecule [43]. Another was in the UV region (354 nm), which was associated with naphthalene ring structure [43]. After 15 min of degradation, the 488 nm peak decreased remarkably, indicating that the conjugate azo structure of Acid Scarlet was destroyed quickly. Moreover, during the degradation, the 354 nm peak disappeared gradually, indicating the naphthalene ring was destroyed, though the H_2O_2 dosage was very low.

Although hydroxyl radicals have very strong oxidizing power and offer potentials of destructing organic pollutants ultimately to water, carbon dioxide, and other harmless small molecules, in most cases, organic compounds can only be mineralized partially

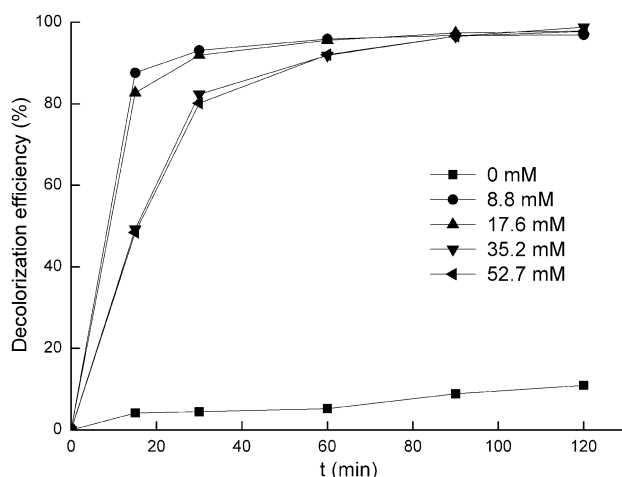


Fig. 8. Effect of H_2O_2 dosage on the degradation of Acid Scarlet (temp. 50°C, dye 200 mg/L, cat. 1 g/L, pH 6.5).

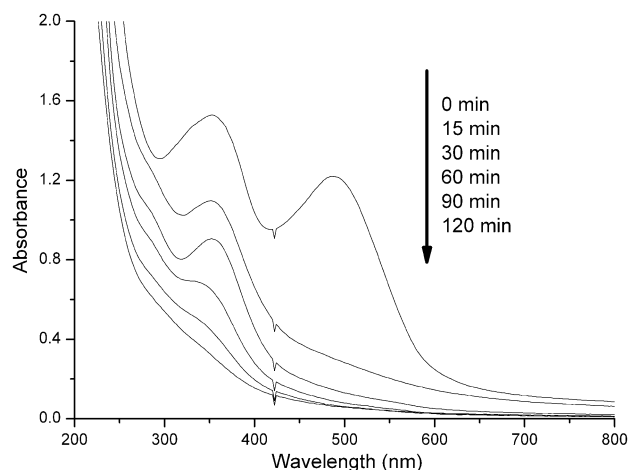


Fig. 9. The UV–visible absorption spectra during the degradation of Acid Scarlet (temp. 50°C, dye 200 mg/L, cat. 1 g/L, H_2O_2 17.6 mM, pH 6.5).

through Fenton or Fenton-like processes. The analysis of intermediates using LC-MS or GC-MS can give clues of degradation mechanics [44,45]. For the degradation of azo dyes, the splitting of nitrogen-to-nitrogen double bonds is relatively easy and the decolorization can be observed. The colorless intermediates such as benzene and naphthalene derivatives are usually more stable, and may be more toxic than the parent molecules [45]. In our study, the change of UV-visible absorption spectra during the dye degradation showed that the conjugate azo structure of Acid Scarlet was split quickly; moreover, most of the naphthalene rings of the intermediates formed from Acid Scarlet were eventually destroyed.

3.2.5. Effect of initial pH

Generally, solution pH influenced significantly not only the degradation of pollutants, but also the leaching of metal species from catalysts. In this study, the effect of pH was examined by adjusting the initial pH of dye solution within the range 4.5–10.5. The results indicated that the Cu-L zeolite could be used in a wide initial pH range, and under near-neutral conditions, the catalyst showed the highest catalytic activity (Fig. 10). In addition, during the degradation, the system pH tended to neuter, whatever the initial pH was (Fig. 11). A near-neutral pH condition is preferable because operation could easily apply to most wastewater. Moreover, acidic conditions would significantly enhance the leaching of metal species from catalysts.

The degradation of azo dyes generally involves the opening of aromatic and naphthalene rings producing organic acids such as formic, acetic, and oxalic acids.

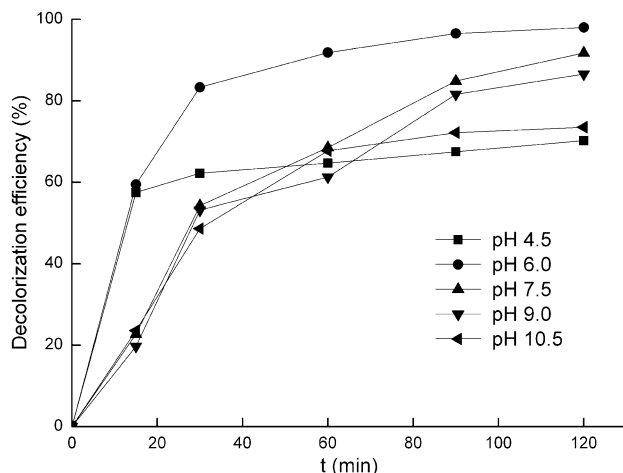


Fig. 10. Effect of initial pH on the degradation of Acid Scarlet (temp. 50°C, dye 400 mg/L, cat. 1 g/L, H₂O₂ 17.6 mM).

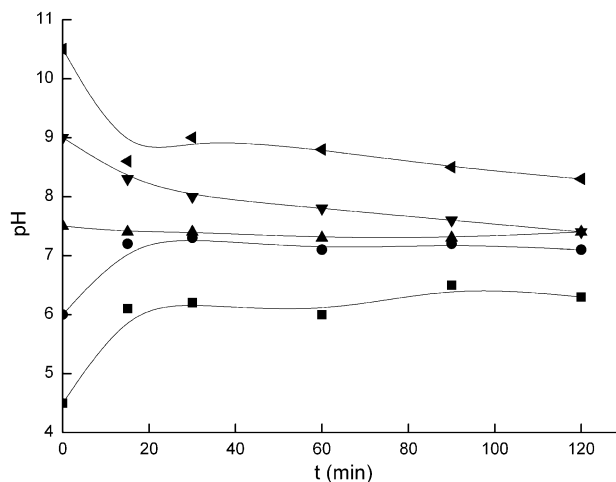


Fig. 11. Change of pH during the degradation of Acid Scarlet (temp. 50°C, dye 400 mg/L, cat. 1 g/L, H₂O₂ 17.6 mM).

Further degradation of these acids is usually difficult, eventually resulting in acid solutions [46]. However, literatures seldom traced the change of solution pH during the dye degradation. Actually, the degradation of azo dyes also produces some basic intermediate compounds such as aromatic amine and ammonia, which may form buffer solutions with acids [47]. This may be an explanation why the system pH tended to neuter during the degradation. This also means that in our degradation the complete mineralization was not reached.

3.2.6. Effect of NaCl and Na₂SO₄

Real dye wastewater usually contains inorganic salts, which may interfere with the peroxide degradation of dyes. This is because hydroxyl radicals are extremely active oxidants and may react with these salts. The oxidant species formed are usually less reactive comparing with the hydroxyl radicals. For example, chloride ions react with hydroxyl radicals to form chlorine radicals. In some cases, the rate of azo dyes reacting with chlorine radicals was 100–1,000 times slower than that with hydroxyl radicals. Even so, the inhibition of inorganic ions depended extremely on the conditions, especially the pH and concentration of ions [48]. Under our experimental conditions, adding NaCl or Na₂SO₄ to 20 g/L in the dye solution obviously decreased the initial rate of Acid Scarlet degradation. However, it did not influence the degradation of Acid Scarlet significantly, because the decolorization efficiencies at 120 min still reached at 95 and 91%, respectively (Fig. 12).

3.3. Stability of catalyst

The long-term stability of a catalyst is extremely important for its practical application. The leaching of metal from catalysts into the acidic reaction medium under Fenton's system is one of the major causes of catalyst deactivation in heterogeneous Fenton's system. To evaluate the stability of the as-synthesized Cu-L zeolite, the Cu concentration of filtrate was measured using an atomic absorption spectrometer after the peroxide degradation of Acid Scarlet. The concentration of leaching Cu measured was only 0.68 mg/L, much lower than many Cu-containing catalysts [15,18,19,21,49]. However, this value was not negligible because it was about 6.8% of Cu content of the catalyst. Consequently, the stability of Cu-L zeolites should still be improved.

3.4. Effect of diffusion and adsorption

Few studies concerned the effect of diffusion and adsorption on the degradation when porous catalysts were used in Fenton's process. However, Gonzalez-Olmos et al. [31] pointed out that the adsorptive enrichment of smaller molecular in the zeolite pore system had a positive effect on the degradation rate. It is worth noting that the channel diameter of zeolite L is 0.71 nm, even less than the critical diameter (0.74 nm) of *m*-xylene [50]. Here the critical diameter is defined as the diameter of the smallest cylinder inside which the molecule will fit. Obviously, Acid Scarlet molecule cannot diffuse into the narrow channels of zeolite Cu-L. According to the mechanism

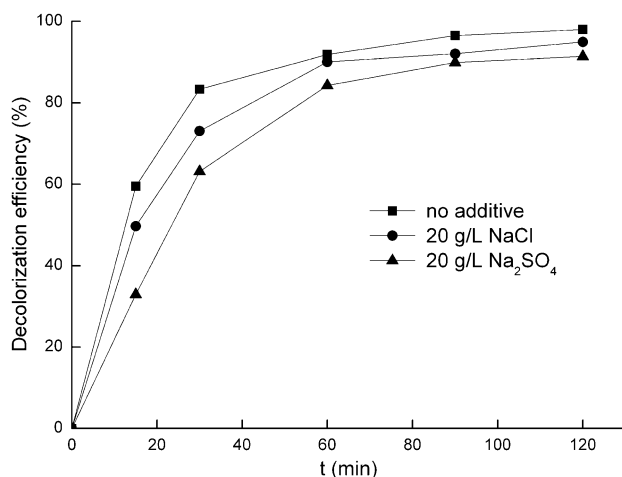


Fig. 12. Effect of NaCl and Na₂SO₄ on the degradation of Acid Scarlet (temp. 50°C, dye 400 mg/L, cat. 1 g/L, H₂O₂ 17.6 mM, pH 6.5).

of heterogeneous Fenton's reaction, H₂O₂ molecules diffuse into the channels of zeolite Cu-L and react with the active sites generating hydroxyl radicals, and then the hydroxyl radicals must diffuse out to degrade the dye. Before diffusing out of channels, partial hydroxyl radicals may disappear by reacting with each other to produce oxygen molecules, or by reacting with some ions such as Cl⁻, CO₃²⁻, and SO₄²⁻ which commonly exist in real industrial wastewater [48]. However, our results suggested that the diffusion limitation did not have significantly negative effects on the dye degradation. The microporous zeolite Cu-L showed considerably high catalytic activity. Moreover, we think that the smaller molecules adsorbed strongly at the inner surface of catalysts can inhibit the generation of hydroxyl radicals. In this occasion, a lower catalytic activity may be observed.

4. Conclusions

By adding Cu salts in the initial gels, a series of Cu-L zeolites with various Cu contents could be synthesized hydrothermally. Adjusting Cu content could result in a high activity catalyst for the degradation of azo dyes, especially with effective use of H₂O₂ and a wide pH range. Cu species highly dispersed in the channels of zeolite L played a crucial role for the catalytic activity. The limitation of diffusion and adsorption of larger dye molecules did not influence the degradation. The catalyst showed the highest catalytic activity under near-neutral conditions. The existence of inorganic salts such as NaCl and Na₂SO₄ obviously decreased the initial rate of Acid Scarlet degradation, but did not influence the eventual decolorization efficiencies significantly. The catalyst appeared to have good stability and less Cu was leached out during the dye degradation. However, the leaching of Cu was ignorable and the improvement of stability of Cu-L zeolite will still be a challenge.

Acknowledgments

The authors thank "NSFC-Henan Talent Development Joint Fund (Grant No. U1204215)" for financial support.

References

- [1] G. Busca, S. Berardinelli, C. Resini, L. Arrighi, Technologies for the removal of phenol from fluid streams: A short review of recent developments, *J. Hazard. Mater.* 160 (2008) 265–288.
- [2] A. Chiavola, *Textiles, Water Environ. Res.* 81 (2009) 1696–1730.

- [3] T.A. Nguyen, R.S. Juang, Treatment of waters and wastewaters containing sulfur dyes: A review, *Chem. Eng. J.* 219 (2013) 109–117.
- [4] M. Pera-Titus, V. García-Molina, M.A. Baños, J. Giménez, S. Esplugas, Degradation of chlorophenols by means of advanced oxidation processes: A general review, *Appl. Catal. B: Environ.* 47 (2004) 219–256.
- [5] A. Vogelpohl, S.M. Kim, Advanced oxidation processes (AOPs) in wastewater treatment, *J. Ind. Eng. Chem.* 10 (2004) 33–40.
- [6] E. Neyens, J. Baeyens, A review of classic Fenton's peroxidation as an advanced oxidation technique, *J. Hazard. Mater.* 98 (2003) 33–50.
- [7] J.J. Pignatello, E. Oliveros, A. Mackay, Advanced oxidation processes for organic contaminant destruction based on the Fenton reaction and related chemistry, *Crit. Rev. Environ. Sci. Technol.* 36 (2006) 1–84.
- [8] P. Bautista, A.F. Mohedano, J.A. Casas, J.A. Zazo, J.J. Rodriguez, An overview of the application of Fenton oxidation to industrial wastewaters treatment, *J. Chem. Technol. Biotechnol.* 83 (2008) 1323–1338.
- [9] J.L. Wang, L.J. Xu, Advanced oxidation processes for wastewater treatment: Formation of hydroxyl radical and application, *Crit. Rev. Environ. Sci. Technol.* 42 (2012) 251–325.
- [10] S. Perathoner, G. Centi, Wet hydrogen peroxide catalytic oxidation (WHPCO) of organic waste in agro-food and industrial streams, *Top. Catal.* 33 (2005) 207–224.
- [11] P.V. Nidheesh, R. Gandhimathi, S.T. Ramesh, Degradation of dyes from aqueous solution by Fenton processes: A review, *Environ. Sci. Pollut. Res.* 20 (2013) 2099–2132.
- [12] M.C. Pereira, L.C. Oliveira, E. Murad, Iron oxide catalysts: Fenton and Fenton like reactions—A review, *Clay Miner.* 47(3) (2012) 285–302.
- [13] R.M. Liou, S.H. Chen, CuO impregnated activated carbon for catalytic wet peroxide oxidation of phenol, *J. Hazard. Mater.* 172 (2009) 498–506.
- [14] J.A. Melero, F. Martínez, J.A. Botas, R. Molina, M.I. Pariente, Heterogeneous catalytic wet peroxide oxidation systems for the treatment of an industrial pharmaceutical wastewater, *Water Res.* 43 (2009) 4010–4018.
- [15] K.M. Valkaj, A. Katović, S. Zrnčević, Catalytic properties of Cu/13X zeolite based catalyst in catalytic wet peroxide oxidation of phenol, *Ind. Eng. Chem. Res.* 50 (2011) 4390–4397.
- [16] A.R. Yeddou, S. Chergui, A. Chergui, F. Halet, A. Hamza, B. Nadjemi, A. Ould-Dris, J. Belkouch, Removal of cyanide in aqueous solution by oxidation with hydrogen peroxide in presence of copper-impregnated activated carbon, *Miner. Eng.* 24 (2011) 788–793.
- [17] N. Inchaurredo, J. Cechini, J. Font, P. Haure, Strategies for enhanced CWPO of phenol solutions, *Appl. Catal. B: Environ.* 111–112 (2012) 641–648.
- [18] N.S. Inchaurredo, P. Massa, R. Fenoglio, J. Font, P. Haure, Efficient catalytic wet peroxide oxidation of phenol at moderate temperature using a high-load supported copper catalyst, *Chem. Eng. J.* 198–199 (2012) 426–434.
- [19] X. Zhong, J. Barbier Jr., D. Duprez, H. Zhang, S. Royer, Modulating the copper oxide morphology and accessibility by using micro-/mesoporous SBA-15 structures as host support: Effect on the activity for the CWPO of phenol reaction, *Appl. Catal. B: Environ.* 121–122 (2012) 123–134.
- [20] O.P. Taran, S.A. Yashnik, A.B. Ayusheev, A.S. Piskun, R.V. Prihod'ko, Z.R. Ismagilov, V.V. Goncharuk, V.N. Parmon, Cu-containing MFI zeolites as catalysts for wet peroxide oxidation of formic acid as model organic contaminant, *Appl. Catal. B: Environ.* 140–141 (2013) 506–515.
- [21] V. Subbaramaiah, V.C. Srivastava, I.D. Mall, Optimization of reaction parameters and kinetic modeling of catalytic wet peroxidation of picoline by Cu/SBA-15, *Ind. Eng. Chem. Res.* 52 (2013) 9021–9029.
- [22] V. Subbaramaiah, V.C. Srivastava, I.D. Mall, Catalytic activity of Cu/SBA-15 for peroxidation of pyridine bearing wastewater at atmospheric condition, *AIChE J.* 59 (2013) 2577–2586.
- [23] A. Rodríguez, G. Ovejero, J.L. Sotelo, M. Mestanza, J. García, Heterogeneous Fenton catalyst supports screening for mono azo dye degradation in contaminated wastewaters, *Ind. Eng. Chem. Res.* 49 (2010) 498–505.
- [24] S. Navalon, A. Dhakshinamoorthy, M. Alvaro, H. Garcia, Heterogeneous Fenton catalysts based on activated carbon and related materials, *ChemSusChem* 4 (2011) 1712–1730.
- [25] L.F. Liotta, M. Gruttadauria, G. Di Carlo, G. Perrini, V. Librando, Heterogeneous catalytic degradation of phenolic substrates: Catalysts activity, *J. Hazard. Mater.* 162 (2009) 588–606.
- [26] E.G. Garrido-Ramírez, B.K.G. Theng, M.L. Mora, Clays and oxide minerals as catalysts and nanocatalysts in Fenton-like reactions—A review, *Appl. Clay Sci.* 47 (2010) 182–192.
- [27] S. Navalon, M. Alvaro, H. Garcia, Heterogeneous Fenton catalysts based on clays, silicas and zeolites, *Appl. Catal. B: Environ.* 99 (2010) 1–26.
- [28] N.R. Sanabria, R. Molina, S. Moreno, Development of pillared clays for wet hydrogen peroxide oxidation of phenol and its application in the posttreatment of coffee wastewater, *Int. J. Photoenergy* 2012 (2012) 1–17.
- [29] Y.C. Yaman, G. Gündüz, M. Dükkancı, Degradation of CI Reactive Red 141 by heterogeneous Fenton-like process over iron-containing ZSM-5 zeolites, *Color Technol.* 129 (2012) 69–75.
- [30] M.L. Rache, A.R. García, H.R. Zea, A.M.T. Silva, L.M. Madeira, J.H. Ramírez, Azo-dye orange II degradation by the heterogeneous Fenton-like process using a zeolite Y-Fe catalyst—Kinetics with a model based on the Fermi's equation, *Appl. Catal. B: Environ.* 146 (2014) 192–200.
- [31] R. Gonzalez-Olmos, U. Roland, H. Toufar, F.D. Kopinke, A. Georgi, Fe-zeolites as catalysts for chemical oxidation of MTBE in water with H₂O₂, *Appl. Catal. B: Environ.* 89 (2009) 356–364.
- [32] S. Fukuchi, R. Nishimoto, M. Fukushima, Q.Q. Zhu, Effects of reducing agents on the degradation of 2, 4, 6-tribromophenol in a heterogeneous Fenton-like system with an iron-loaded natural zeolite, *Appl. Catal. B: Environ.* 147 (2014) 411–419.
- [33] A.V. Russo, L.F. Torriggia, S.E. Jacobo, Natural clinoptilolite-zeolite loaded with iron for aromatic hydrocarbons

- removal from aqueous solutions, *J. Mater. Sci.* 49 (2014) 614–620.
- [34] Ch. Baerlocher, L.B. McCusker, D.H. Olson, Atlas of Zeolite Framework Types, sixth ed., Elsevier, Amsterdam, 2007.
- [35] Y.S. Ko, W.S. Ahn, Hydrothermal synthesis of zeolite L in a Na^+/K^+ mixed alkali system, *Korean J. Chem. Eng.* 25 (2008) 1546–1552.
- [36] P.N. Joshi, S.V. Awate, V.P. Shiralkar, Partial isomorphous substitution of iron(3+) in the LTL framework, *J. Phys. Chem.* 97 (1993) 9749–9753.
- [37] E.M. Flanigen, H. Khatami, Infrared structural studies of zeolite frameworks, in: E.M. Flanigen, L.B. Sand (Eds.), *Molecular Sieves Zeolites I*, American Chemical Society, Washington, DC, 1971, pp. 201–229.
- [38] A.P.L. Batista, H.W.P. Carvalho, G.H.P. Luz, P.F.Q. Martins, M. Gonçalves, L.C.A. Oliveira, Preparation of CuO/SiO_2 and photocatalytic activity by degradation of methylene blue, *Environ. Chem. Lett.* 8 (2010) 63–67.
- [39] M.L. Luo, D. Bowden, P. Brimblecombe, Catalytic property of Fe–Al pillared clay for Fenton oxidation of phenol by H_2O_2 , *Appl. Catal. B: Environ.* 85 (2009) 201–206.
- [40] Y.Z. Zhan, X. Zhou, B. Fu, Y.L. Chen, Catalytic wet peroxide oxidation of azo dye (Direct Blue 15) using solvothermally synthesized copper hydroxide nitrate as catalyst, *J. Hazard. Mater.* 187 (2011) 348–354.
- [41] P. Shukla, S.B. Wang, H.Q. Sun, H.M. Ang, M. Tadé, Adsorption and heterogeneous advanced oxidation of phenolic contaminants using Fe loaded mesoporous SBA-15 and H_2O_2 , *Chem. Eng. J.* 164 (2010) 255–260.
- [42] H. Hassan, B.H. Hameed, Fe-clay as effective heterogeneous Fenton catalyst for the decolorization of reactive blue 4, *Chem. Eng. J.* 171 (2011) 912–918.
- [43] K. Hirayama, *Handbook of Ultra Violet and Visible Absorption Spectra of Organic Compounds*, Springer-Verlag, New York, NY, 1967.
- [44] S. Hisaindee, M.A. Meetani, M.A. Rauf, Application of LC-MS to the analysis of advanced oxidation process (AOP) degradation of dye products and reaction mechanisms, *Trends Anal. Chem.* 49 (2013) 31–44.
- [45] S. Rismayani, M. Fukushima, H. Ichikawa, K. Tatsumi, Decolorization of orange II by catalytic oxidation using iron (III) phthalocyanine-tetrasulfonic acid, *J. Hazard. Mater.* 114 (2004) 175–181.
- [46] C. Hu, J.C. Yu, Z.P. Hao, P.K. Wong, Photocatalytic degradation of triazine-containing azo dyes in aqueous TiO_2 suspensions, *Appl. Catal. B: Environ.* 42 (2003) 47–55.
- [47] S. Hisaindee, M.A. Meetani, M.A. Rauf, Application of LC-MS to the analysis of advanced oxidation process (AOP) degradation of dye products and reaction mechanisms, *Trends Anal. Chem.* 49 (2013) 31–44.
- [48] I. Arslan-Alaton, A review of the effects of dye-assisting chemicals on advanced oxidation of reactive dyes in wastewater, *Color Technol.* 119 (2003) 345–353.
- [49] T. Granato, A. Katovic, K. Maduna Valkaj, A. Tagarelli, G. Giordano, Cu-silicalite-1 catalyst for the wet hydrogen peroxide oxidation of phenol, *J. Porous Mater.* 16 (2009) 227–232.
- [50] V.R. Choudhary, V.S. Nayak, T.V. Choudhary, Single-component sorption/diffusion of cyclic compounds from their bulk liquid phase in H-ZSM-5 zeolite, *Ind. Eng. Chem. Res.* 36 (1997) 1812–1818.